How Flexible Is the Furanose Ring? 1. A Comparison of Experimental and Theoretical Studies

Wilma K. Olson*[1] and Joel L. Sussman[2]

*Contribution from the Department of Chemistry, Rutgers University,
New Brunswick, New Jersey 08903, and the Department of Structural Chemistry,
The Weizmann Institute of Science, Rehovot, Israel. Received November 25, 1980*

Abstract: A series of statistical computations have been carried out to test various theoretical potential energy estimates of furanose pseudorotation. Energy surfaces describing the flexibility of both ribose and deoxyribose have been compared through a Boltzmann analysis with each other and also with published X-ray and NMR measurements of pseudorotation (i.e., with distributions of solid state puckerings, standard valence angle geometries, and mean vicinal coupling constants in RNA and DNA analogues). No single theoretical approach is able to account simultaneously for the experimental properties of both ribose and deoxyribose. Methods generally satisfactory for ribose pseudorotation are unsuitable for deoxyribose and vice versa. In the commonly occurring mononucleosides and -nucleotides the pseudorotational motions are decidedly "stiff" with the potential energy barrier somewhat higher for ribose than for deoxyribose. When incorporated into a polynucleotide backbone, this local stiffness is a major determinant of chain flexibility and a characteristic difference between RNA and DNA systems.

The furanose is the essential link that joins the negatively charged phosphates and the heterocyclic bases into the unique chemical framework of a polynucleotide. The inherent flexibility of the sugar introduces major structural changes in the naturally occurring nucleic acids and has an important bearing on their biological function. According to extensive X-ray crystallographic studies of low molecular weight nucleic acid analogues (e.g., monomers and short oligomers), the pentose ring adopts one of two principal puckered shapes.[3] The two basic forms (C_3-endo and C_2-endo or a minor variant) characterize two distinctly different families (A and B) of nucleic acid structures[4] and produce a wide variety of double-helical models.[5]

Both solid-state[6-9] and solution[10-13] studies suggest that the interconversion between the two puckered states of the pentose occurs via a pseudorotation pathway of closely related intermediate forms rather than through a planar ring structure. The pucker moves continuously around the five-membered system with neighboring atoms displaced alternately above and below a mean ring plane. In contrast to the unsubstituted cyclopentane ring where the interconversion of puckered states occurs without significant energetic effects,[14] the presence of endocyclic and exocyclic substituents in the pentose moiety introduces a potential barrier that opposes free pseudorotation. In view of the very few X-ray crystallographic examples of intermediate ring puckering,[15-21] one

generally expects the pseudorotation barrier in furanose to be sufficiently high (i.e., greater than 2 kcal/mol) to suppress intermediate forms. On the other hand, the rapid interconversion of puckered states observed in proton magnetic resonance (^{1}H NMR) studies[11-13,22-29] of model nucleosides and nucleotides limits the magnitude of the pseudorotation barrier to fairly low levels (i.e., less than 5 kcal/mol).

A sophisticated potential energy analysis by Levitt and Warshel[30] has recently challenged the traditional views of pentose flexibility. According to their study, the interconversion between puckered forms of both ribose and deoxyribose is close to free and the pentose is termed "the most flexible degree of freedom in the nucleic acid chain". This extreme flexibility leads, in turn, to an unusual model of smoothly bent DNA involving exaggerated propeller-like twisting of base pairs[31] and suggests similar behavior in RNA. With the exception of a recent Hückel analysis by Beckel and Hashemi-Attar[32] that supports the "free" motion of sugars, other theoretical groups[33-38] predict the pseudororation potential

(1) Rutgers University. U.S.P.H.S. Research Career Development Awardee.

(2) Weizmann Institute.

(3) M. Sundaralingam in "The Jerusalem Symposia on Quantum Chemistry and Biochemistry", Vol. 5, E. D. Bergmann and B. Pullman, Eds., The Israel Academy of Sciences and Humanities, Jerusalem, 1973, pp 417–455.

(4) R. Chandrasekaran, S. Arnott, A. Banerjee, S. Campbell-Smith, A. G. Leslie, and L. Puigjaner, *ACS Symp. Ser.* No. **141**, 483–502 (1980).

(5) S. Arnott, R. Chandrasekaran, P. J. Bond, D. L. Birdsall, A. G. W. Leslie, and L. C. Puigjaner, "Proceedings of the Seventh Aharon Katzir-Katchalsky Conference on Structural Aspects of Recognition and Assembly in Biological Macromolecules", Nof Ginossar, Israel, 1980.

(6) C. Altona and M. Sundaralingam, *J. Am. Chem. Soc.*, **94**, 8205–8212 (1972).

(7) P. Murray-Rust and S. Motherwell, *Acta Crystallogr., Sect. B*, **B34**, 2534–2546 (1978).

(8) H. P. M. de Leeuw, C. A. G. Haasnoot, and C. Altona, *Isr. J. Chem.*, **20**, 108–126 (1980).

(9) E. Westhof and M. Sundaralingam, *J. Am. Chem. Soc.*, **102**, 1493–1500 (1980).

(10) C. Altona and M. Sundaralingam, *J. Am. Chem. Soc.*, **95**, 2333–2344 (1973).

(11) D. B. Davis and S. S. Danyluk, *Biochemistry*, **13**, 4417–4434 (1974).

(12) D. B. Davis and S. S. Danyluk, *Biochemistry*, **14**, 543–554 (1975).

(13) F. E. Evans and R. H. Sarma, *Nature (London)*, **263**, 567–572 (1976).

(14) D. Cremer and J. A. Pople, *J. Am. Chem. Soc.*, **97**, 1358–1367 (1975).

(15) J. Konnert, I. L. Karle, and J. Karle, *Acta Crystallogr., Sect. B*, **B26**, 770–778 (1970).

(16) D. W. Young, P. Tollin, and H. R. Wilson, *Acta Crystallogr., Sect. B*, **B30**, 2012–2018 (1974).

(17) M. A. Viswamitra, T. P. Seshadri, and M. L. Post, *Nature (London)*, **258**, 542–544 (1975).

(18) P. Narayanan and H. M. Berman,, *Carbohydr. Res.*, **44**, 169–180 (1975).

(19) B. E. Fischer and R. Bau, *J. Chem. Soc., Chem. Commun.*, 272–273 (1977).

(20) A. Grand and J. Cadet, *Acta Crystallogr., Sect. B*, **B34**, 1524–1528 (1978).

(21) G. I. Birnbaum, T.-S. Lin, G. T. Shiau, and W. H. Prusoff, *J. Am. Chem. Soc.*, **101**, 3352–3358 (1979).

(22) F. E. Hruska, A. A. Grey, and I. C. P. Smith, *J. Am. Chem. Soc.*, **92**, 214–215 (1970).

(23) F. E. Hruska, *J. Am. Chem. Soc.*, **93**, 1795–1797 (1971).

(24) H. Dugas, B. J. Blackburn, R. K. Robins, R. Deslauriers, and I. C. P. Smith, *J. Am. Chem. Soc.*, **93**, 3468–3470 (1971).

(25) T. Schleich, B. J. Blackburn, R. D. Lapper, and I. C. P. Smith, *Biochemistry*, **11**, 137–145 (1972).

(26) B. P. Cross and T. Schleich, *Biopolymers*, **12**, 2381–2389 (1973).

(27) F. E. Hruska, D. J. Wood, and K. K. Ogilvie in "Structure and Conformation of Nucleic Acids and Protein-Nucleic Acid Interactions", M. Sundaralingam and S. T. Rao, Eds., University Park Press, Baltimore, Md., 1975, pp 597–611.

(28) A. L. George, F. E. Hruska, K. K. Ogilvie, and A. Holy, *Can. J. Chem.*, **56**, 1170–1176 (1978).

(29) W. Guschlbauer and K. Jankowski, *Nucleic Acids Res.*, **8**, 1421–1433 (1980).

(30) M. Levitt and A. Warshel, *J. Am. Chem. Soc.*, **100**, 2607–2613 (1978).

(31) M. Levitt, *Proc. Natl. Acad. Sci. U.S.A.*, **75**, 640–644 (1978).

(32) C. L. Beckel and A.-R. Hashemi-Attar in "Biomolecular Structure, Conformation, Function, and Evolution", Vol. 2, R. Srinivasan, E. Subramanian, and N. Yathindra, Eds., Pergamon Press, Oxford, 1981, pp 305–310.

(33) A. A. Lugovskoi and V. G. Dashevskii, *Mol. Biol. (Engl. Transl.)*, **6**, 354–360 (1972).

(34) V. Sasisekharan in "The Jerusalem Symposia on Quantum Chemistry and Biochemistry", Vol. 5, E. D. Bergmann and B. Pullman, Eds., The Israel Academy of Sciences and Humanities, Jerusalem, 1973, pp 247–260.

(35) A. Saran, D. Perahia, and B. Pullman, *Theor. Chim. Acta*, **30**, 31–44 (1973).

energy barrier to be much higher than the 0.5-kcal/mol value reported by Levitt and Warshel. Furthermore, Röder et al.[39] have claimed to measure an energy barrier to pseudorotation of 4.7 ± 0.5 kcal/mol from ^{13}C relaxation studies of purine ribonucleosides. In addition, numerous researchers[40-46] (both theoretical and experimental) have concluded that the phosphodiester constitutes a greater source of flexibility than the sugar in the polynucleotide backbone (i.e., the phosphodiester is a more mobile moiety that moves over much wider ranges of conformation space). Moreover, one can build smoothly bent models of DNA without invoking the occurrence of unusual sugar puckering.[47-52]

Unfortunately, a complete description of pseudorotation in either ribose or deoxyribose is not easily derivable from experimental observations alone. It is therefore necessary to rely upon theoretical potential energy estimates to bridge the gaps between experimental examples. In view of the above cited disparities among the various theoretical studies of pseudorotation, it is especially important to recognize the extent of reliability of different computational schemes. A suitable potential function is expected to reproduce all relevant experimental data, including not only potential barriers but also conformer populations of both deoxyribose and ribose.[53] A scheme that meets these criteria, in addition, is likely to provide information useful in understanding the properties of these molecules in terms of their chemical architecture.

As part of an effort to comprehend the nature of sugar flexibility in the nucleic acids, we have examined in detail the available potential energy surfaces of pentose pseudorotation. From the reported energies we derive statistical weights and then compare the theoretical data with each other and also with published X-ray and NMR data (i.e., with distributions of solid-state structures, standard pentose geometries, and mean vicinal coupling constants). Unfortunately, we find no single theoretical approach that accounts in every respect for the experimental properties of the commonly occurring nucleosides and nucleotides. Methods generally satisfactory for ribose pseudorotation fail to reproduce the conformational preferences of deoxyribose; other potentials that mimic the deoxyribose data predict unusual behavior in ribose. In addition, there appears to be no possibility of reconciling the flat energy surfaces characterizing "free" pseudorotation with either solid-state or solution studies of model nucleic acids. This unusual conformational prediction may reflect the distorted structural
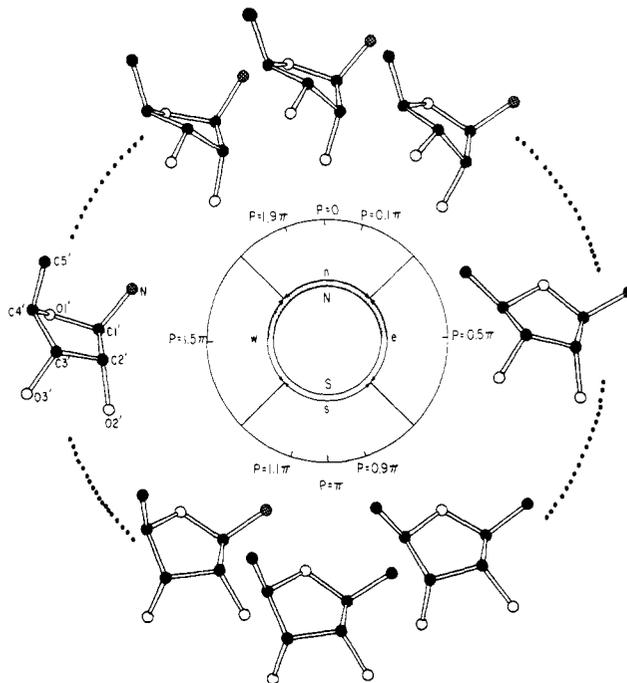

Figure 1. Schematic illustrating the pseudorotation cycle of a simple ribose sugar with $\tau_m{}^0 = 38°$. Each puckered form is distinguished by its phase angle P in radians. Atoms are designated on the $P = 1.5\pi$ puckered form. The pseudorotation wheel is divided into four quadrants (n, e, s, and w) associated with minima and maxima reported in potential energy studies. The N/S pseudorotation ranges introduced by Altona and Sundaralingam[6] are distinguished from our four ranges along the inner circle of the figure.

geometries (i.e., involving anomalous valence bond angles) utilized in the respective calculations. As we explain elsewhere,[54] "free" pseudorotation may very likely predominate in certain chemically unusual nucleic acids. In normal DNA and RNA analogues, however, the pseudorotational motions are decidely "stiff" with the potential energy barrier somewhat higher for ribose than for deoxyribose. Such "stiff" local motions ultimately determine the flexibility of the polynucleotide as a whole and the conformational differences between naturally occurring RNA and DNA.

Pseudorotation Geometry

The pseudorotation of the furanose is conveniently described, following Altona and Sundaralingam,[6] by two mathematical parameters—τ_m, the amplitude of puckering, and P, the phase angle of pseudorotation. The conformations of the five ring torsion angles are related to τ_m and P through the simple trigonometric expression

$$\tau_j = \tau_m \cos (P + 0.8\pi(j - 2)) \qquad (1)$$

The τ_j values, where $j = 0-4$, are expressed in degrees and are defined with respect to cis = 0° rotations about bonds $O_{1'}-C_{1'}$, $C_{1'}-C_{2'}$, $C_{2'}-C_{3'}$, $C_{3'}-C_{4'}$, and $C_{4'}-O_{1'}$, respectively, of the pentose ring (cf. Figure 1). According to the large body of X-ray crystallographic data[6-9] and also following potential energy analyses,[30,32-36] the τ_m of ribose and deoxyribose are confined to a relatively narrow range centered approximately at 40°. The parameter P in eq 1 is defined with respect to a standard pucker where $\tau_2 = \tau_m$. In the furanose this reference ($P = 0$) state is the symmetrical twist conformation shown in Figure 1 with atoms $C_{2'}$ and $C_{3'}$ displaced respectively below and above the plane defined by the three remaining ring atoms. P is expressed here in radians to avoid any confusion between the two angular variables of pseudorotation.

As P increases from 0, the ring passes at increments of 0.2π rad through ten distinct twist (T) forms. Midway between the T states, the ring adopts ten different envelope (E) states, including

(36) Unpublished data of T. Sato, V. Sasisekharan, and R. Langridge as cited by S. Broyde et al.[37,38] and communicated personally by S. Broyde.

(37) S. Broyde, R. M. Wartell, S. D. Stellman, and B. Hingerty, *Biopolymers*, **17**, 1485–1506 (1978).

(38) S. Broyde and B. Hingerty, in "Stereodynamics of Molecular Systems", R. H. Sarma, Ed., Pergamon Press, New York, 1979, pp 351–366.

(39) O. Röder, H.-D. Lüdemann, and E. von Goldanmer, *Eur. J. Biochem.*, **53**, 517–525 (1975).

(40) S.-H. Kim, H. M. Berman, N. C. Seeman, and M. D. Newton, *Acta Crystallogr. Sect. B*, **B29**, 703–710 (1973).

(41) M. Sundaralingam, in "Structure and Conformation of Nucleic Acids and Protein-Nucleic Acid Interactions", M. Sundralingam and S. T. Rao, Eds., University Park Press, Baltimore, Md., 1975, pp 487–524.

(42) D. J. Patel and L. Canuel, *Proc. Natl. Acad. Sci. U.S.A.*, **73**, 674–678 (1976).

(43) C.-H. Lee, F. S. Ezra, N. S. Kondo, R. H. Sarma, and S. S. Danyluk, *Biochemistry*, **15**, 3627–3639 (1976).

(44) P. J. Cozzone and O. Jardetzky, *Biochemistry*, **15**, 4853–4859, 4860–4865 (1976).

(45) N. Yathindra and M. Sundaralingam, *Proc. Natl. Acad. Sci. U.S.A.*, **71**, 3325–3328 (1974).

(46) W. K. Olson, *Biopolymers*, **14**, 1775–1795 (1975).

(47) N. Z. Namaradze, A. V. Goryunov, and T. M. Birshtein, *Biophys. Chem.*, **7**, 59–70 (1977).

(48) J. L. Sussman and E. Trifonov, *Proc. Natl. Acad. Sci. U.S.A.*, **75**, 103–107 (1978).

(49) V. Sasisekharan, N. Pattabiraman, and G. Gupta, *Proc. Natl. Acad. Sci. U.S.A.*, **75**, 4092–4096 (1978).

(50) W. K. Olson, *Biopolymers*, **18**, 1235–1260 (1979).

(51) V. B. Zhurkin, Yu. P. Lysov, and V. I. Ivanov, *Nucleic Acids Res.*, **6**, 1081–1096 (1979).

(52) N. Yathindra, *Curr. Sci.*, **48**, 753–756 (1979).

(53) Although packing may play a part in some particular structures, the X-ray crystallographic data taken as a whole should give a good statistical estimate of the population.

(54) W. K. Olson, *Nucleic Acids Res.*, **9**, 1251–1262 (1981).

the predominant $C_{3'}$-endo or ^3E and $C_{2'}$-endo or ^2E conformers cited above at $P = 0.1\pi$ and 0.9π rad, respectively. The various T and E conformations of the furanose fall naturally into four distinct conformational categories and pseudorotation space divides conveniently into four equally sized quadrants. The northern (n) and southern (s) quadrants centered respectively at $P = 0$ and π rad comprise the two predominant categories of observed sugar puckering (i.e., ^3E and ^2E, respectively). The eastern (e) quadrant centered about $P = 0.5\pi$ rad includes the intermediate $O_{1'}$-endo or $_oE$ conformer (cf. Figure 1) reported in a few X-ray structures[5-21] while the western (w) quadrant centered at $P = 1.5\pi$ rad contains the sterically encumbered (and, as yet for furanose, experimentally unobserved $O_{1'}$-exo or $_oE$ puckering (see Figure 1)).[55] Pseudorotation space, as previously described by Altona and Sundaralingam,[6,10] involves two major domains termed N and S. The N range centered at $P = 0$ contains the n quadrant defined here and the northern halves of the intermediate e and w quadrants; the S region similarly encompasses the s quadrant defined here and the remaining halves of the e and w quadrants. We detail the differences between the N/S and n, e, s, and w descriptions of pseudorotation space in Figure 1. As demonstrated below, our quadrant nomenclature helps to analyze the potential barrier of pentose pseudorotation and hence to differentiate the "free" and "stiff" puckering motions predicted by different energy studies.

Statistical Weight Analysis

Differences among the various theoretical studies of furanose pseudorotation are not readily apparent from potential energy diagrams which, on this account, are not reported here. The differences are more easily distinguished from the relative statistical weights σ_q associated with the four distinct quadrants of pseudorotation space. These values are the fractional contribution of all conformers within each quadrant q to the configurational partition function $z_{\tau_m,P}$ for the entire $V(\tau_m,P)$ potential energy surface. The partition function is obtained by integration of the Boltzmann factors of potential energy over all τ_m and P yielding

$$z_{\tau_m,P} = \int_{\tau_m=0}^{\tau_m} \int_{P=0}^{2\pi} \exp(-V(\tau_m,P)/RT) \, d\tau_m \, dP \quad (2)$$

Since τ_m is approximately constant at τ_m^0 for furanose,[6-9] the partition function can be simplified to an integration over P alone with

$$z_P = \int_{P=0}^{2\pi} \exp(-V(\tau_m^0,P)/RT) \, dP \quad (3)$$

and the statistical weights can be expressed as

$$\sigma_q = \frac{\int_q \exp(-V(\tau_m^0,P)/RT) \, dP}{z_P} \quad (4)$$

The integral appearing in the numerator of eq 4 is evaluated over all P within pseudorotation quadrant q.

Inasmuch as values of potential energy are computed at finite values of P, it is not possible in practice to evaluate eq 4. The stipulated integrals must be approximated by the summation of Boltzmann factors over an appropriate set of discrete conformations. Where numerical values of energies are unreported, relative values also must be estimated by interpolation from the published potential surfaces. Exact numerical data when available are found not to differ appreciably from statistical weights obtained by this second approximation.[46]

Theory vs. Experiment in the Solid State

Ribose. Statistical weights describing the pseudorotation of ribose according to several theoretical schemes[30,32,33,35,36] are listed in Table I. The σ_q values are computed, following eq 4, at intervals of 0.1π rad in P corresponding to the ten T and ten E conformations of the sugar ring. The various studies are char-

(55) The chemically constrained 2′,3′-cyclophosphorothioate-U (uridine) molecule is found in the w quadrant of conformation space (W. Saenger and F. Eckstein, *J. Am. Chem. Soc.*, **90**, 4712–4718 (1970)). Such cyclizations, however, are not normally present in furanose rings.

Table I. Comparative Statistical Weights of Pseudorotation in Ribose

method	τ_m^0, deg	system $R_{4'}$	$R_{1'}$	pop. σ_n	σ_e	σ_s	σ_w
PCILO[35,a]	39	CH_2OH	purine	0.13	0.01	0.86	0
	39	CH_2OH	pyrimidine	0.84	0	0.16	0
SE1[33]	40	H	NH_2	0.98	0.02	0	0
SE2[36]	41	CH_2	NH_2	0.46	0.04	0.48	0.02
CFF[30]	40	CH_3	NH_2	0.39	0.33	0.25	0.03
H[32,b]		CH_3	NH_2	0.16	0.64	0.17	0.03
X-ray data[6,9,c]				0.44	0.01	0.55	0

^{a} Statistical weights were estimated as a function of P from the published $V(P,\chi)$ potential surfaces at values of χ that minimized the potential energy. ^{b} Ring puckering was described, following Cremer and Pople,[14] in terms of the maximum deviation $z^0 = 0.4$ Å from a mean ring plane. ^{c} A bibliography of 108 recent ribose structures is given in Table I-S of the supplementary material. A similar compilation of 102 ribose structures was recently reported by de Leeuw et al.[8]

Table II. Comparative Statistical Weights of Pseudorotation in Deoxyribose

method	τ_m^0, deg	system $R_{4'}$	$R_{1'}$	pop. σ_n	σ_e	σ_s	σ_w
PCILO[35,a]	39	CH_2OH	purine	0.11	0.01	0.88	0
	39	CH_2OH	pyrimidine	0.45	0.01	0.54	0
SE2[33]	41	CH_3	NH_2	0.51	0.06	0.38	0.05
CFF[30]	40	CH_3	NH_2	0.39	0.33	0.25	0.03
H[32,b]		CH_3	NH_2	0.10	0.66	0.23	0.01
X-ray data[6,9,c]				0.23	0.10	0.67	0

^{a,b} See corresponding footnotes to Table I. ^{c} A bibliography of 27 recent deoxyribose structures is given in Table II-S of the supplementary material. A similar list of 23 deoxyribose fragments was recently reported by de Leeuw et al.[8]

acterized by the computational procedure, the chemical model under investigation, and the fixed value of τ_m^0. The chemical model is determined by the particular atomic substituents attached to atoms $C_{4'}$ and $C_{1'}$. Also listed in Table I are conformational frequencies of pseudorotation based upon a compilation of relevant X-ray data (108 ribose structures). The solid-state data are divided almost evenly between the n and s quadrants with the s domain somewhat more predominant. In contrast to the predictions of both the consistent force field (CFF) minimization by Levitt and Warshel[30] and the Hückel (H) energy gradient computation by Beckel and Hashemi-Attar,[32] only two examples of the intermediate e range[18,19] of ribose have been recorded to date. (Interestingly, these two X-ray structures are chemically unusual species, one[18] involving a rare base and the other[19] a transition-metal complex.) In the CFF and H studies the low 0.5–0.6-kcal/mol $O_{1'}$-endo energy barrier is primarily responsible for the large statistical weight of the e domain; the unusually high value of $\sigma_e = 0.64$ in the H study is a further consequence of misplaced global energy minima at $P = 0.27\pi$ and 0.74π rad. As evident from Table I, the n/s conformer distribution of crystalline ribose is best approximated by the semiempirical calculations of Sato et al.[36] (SE2). The correct n/s ratio is also predicted by the H calculations if the σ_e states are ignored. The pseudorotation populations predicted by the earlier semiempirical study of Lugovskoi and Dashevskii[33] (SE1) and the PCILO quantum mechanical analysis of Saran et al.[35] are clustered in one or the other of the two experimentally observed domains. Moreover, according to the PCILO approach, the n/s distribution is determined by the nature of the attached base; there is no available experimental evidence, however, that supports a correlation between ring puckering and base sequence in the commonly occurring ribonucleosides and -nucleotides.[6,8-13] A marked bias against the sterically hindered conformers of the w quadrant is the one feature common to all pseudorotation studies of ribose and also in

How Flexible Is the Furanose Ring

J. Am. Chem. Soc., Vol. 104, No. 1, 1982 273

agreement with experimental data.

Deoxyribose. The theoretical data describing the pseudorotation of deoxyribose are compared with each other and with available solid-state data in Table II. Only the PCILO purine study is found to reproduce the strong experimental preference for s-type conformers in the 27 sets of available X-ray data.[6,8,9,15–17,20,21] The PCILO pyrimidine system is divided approximately evenly between n and s domains while the SE2 analysis is biased slightly toward the n range. Unfortunately, deoxyribose was not treated in the SE1 study. In accordance with the X-ray data,[6,8,9,15–21] the statistical weight associated with intermediate e puckering in the PCILO, SE2, and H schemes is increased for deoxyribose compared to ribose. One must recognize, however, that three of the five crystallographic structures of deoxyribose found in the e domain entail rare bases[15,20,21] that may possibly induce the unusual geometry. Furthermore, the e-puckered form of 5'-dUMP[17] lies just inside the $P = 0.75\pi$-rad border with the s quadrant of pseudorotation space. The dG structure[16] is the only commonly occurring furanose in the e-puckering domain. Nevertheless, values of σ_e predicted by the CFF and H approaches are significantly greater than the experimental frequencies. Despite the inconsistency in σ_e, the H data, with minimum energy at $P = 0.75\pi$ rad are seen to reproduce the experimental preference for s over n puckering. Unfortunately, it is not possible to reconcile any aspect of the solid-state behavior of deoxyribose with the predictions of the CFF computations.

Average Coupling Constants

The conformation of the furanose in dilute solution appears to be a blend of puckered states. No single state on the pseudorotation pathway can account for the observed three-bond proton NMR coupling constants (J_{HH}). The couplings between transoidal protons (located on opposite sides of the furanose ring) apparently follow a Karplus-like relationship[56,57]

$$J_{HH} = A \cos^2 \phi + B \cos \phi + C \tag{5}$$

where ϕ is the dihedral angle between the given pair of protons and A, B, and C are constants. Since ϕ is a continuous function of ring puckering, J depends ultimately upon the phase angle of pseudorotation. Conformational analysis based upon a Karplus relationship, however, fails to account for the observed couplings between cisoidal protons (located on the same side) of the furanose.[58] According to recent quantum mechanical simulations in arabinose models,[58,59] there is no unique relationship between J and ϕ in these cases. The cisoidal couplings depend in a complicated fashion upon both the chemical architecture and the conformation (i.e., P) of the whole molecule. The widely applied procedure of accounting for chemical effects by either subtracting a constant value from or multiplying a specific factor with the cisoidal J value obtained by Karplus theory can sometimes lead to serious errors.[58]

The various pseudorotation potential energy estimates described above may be further tested by comparing observed coupling constants with mean values calculated on the basis of theoretical data. The NMR data are usually interpreted in terms of the two predominant X-ray conformers (n and s) without regard to the intermediate forms (e and w) predicted by theory.[10–13,22–29] Statistical mechanical $\langle J_{HH} \rangle$ values may also be evaluated by using the expression

$$\langle J_{HH} \rangle = \frac{\int_{P=0}^{2\pi} J_{HH}(P) \exp(-V(\tau_m^0, P)) \, dP}{z_P} \tag{6}$$

where $J_{HH}(P)$ is a unique function for each pair of protons in the furanose and z_P is given by eq 3. Values of $\langle J_{HH} \rangle$ obtained in
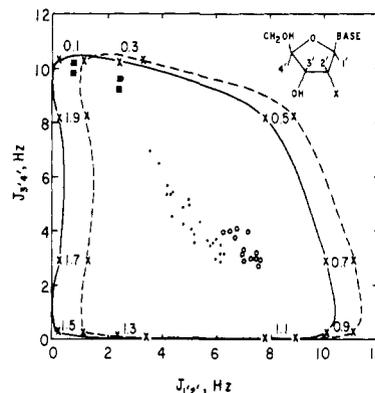

Figure 2. Theoretical dependence of the transoidal proton coupling constants $J_{1'2'}$ and $J_{3'4'}$ upon P in ribose (solid path) and deoxyribose (dashed path). Values of P/π corresponding to a pair of constants are denoted by X. Experimental data are distinguished by darkened circles (ribose), open circles (deoxyribose), and darkened squares (3'–5' cyclic monophosphates of both ribose and deoxyribose). Relevant protons are designated by the chemical structure. The X on the structure may be OH (in ribose) or H (deoxyribose).

this manner are dependent upon the entire pseudorotation potential rather than upon a limited range of states.

The predicted variation of the two transoidal furanose coupling constants $J_{1'2'}$ and $J_{3'4'}$ with P is represented in Figure 2. These values are obtained for ribose, following Dhingra and Sarma,[60] using eq 5 with $A = 10.5$, $B = 1.2$, and $C = 0$ and ϕ chosen in accordance with available X-ray data. It is necessary, however, to use a value of $C = 1$ in the computation of the deoxyribose $J_{1'2'}$ value to take account of the known electronegativity effects involving loss of the 2'-hydroxyl.[10,11] Small variations in A, B, and C and minor angular changes in ϕ are not sufficient to alter the general conclusions described below. Values of P/π corresponding to the ten E conformers along the pseudorotation path are noted by X at the appropriate coordinates on Figure 2. The motion of the ribose is given by the solid curve and that of deoxyribose by the dashed curve. The coupling constants measured for the sugars of various nucleosides and nucleotides[10–13,22–29,61,62] are also designated on the diagram; the ribose data are represented by darkened circles and the deoxyribose data by open circles. The experimental values clustered in the region centered at $J_{1'2'} \approx 1–2$ Hz and $J_{3'4'} \approx 9–10$ Hz (darkened squares) are associated with conformationally constrained 3'–5' cyclic monophosphates;[26,61,62] the solution conformation of the cyclic compounds is apparently similar to the $P \approx 0.2\pi$-rad puckering observed in solid-state studies.[6–9] In the absence of solid-state NMR data, these rigid molecules are the only models available to calibrate the theoretical coupling relationships. The coupling constants of the unconstrained sugars are centrally located with respect to the path of pseudorotation in Figure 2; the blend of conformations describing ribose in solution is more varied and also clearly different from that describing deoxyribose. Because of the intermediate magnitudes of $J_{1'2'}$ and $J_{3'4'}$, numerous combinations of n, e, s, and w populations are expected to reproduce these data.

The different pseudorotational behavior of the cisoidal constant $J_{2'3'}$ in ribose and deoxyribose systems is illustrated in Figure 3. For clarification purposes, $J_{2'3'}$ is taken as the abscissa and P/π as the ordinate in the figure. The theoretical variation of ribose coupling is represented by the solid curve and that of deoxyribose by the dashed curve; experimental data describing the two systems are represented by the bar graphs drawn at the appropriate locations of $J_{2'3'}$. The ribose data are given in blocked format and

(56) M. Karplus, *J. Chem. Phys.*, **30**, 11–15 (1959).

(57) C. Altona, H. R. Buys, H. J. Hageman, and E. Havigna, *Tetrahedron*, **23**, 2265–2279 (1967).

(58) A. Jaworski, I. Ekiel, and D. Shugar, *J. Am. Chem. Soc.*, **100**, 4357–4361 (1978).

(59) A. Jaworski and I. Ekiel, *Int. J. Quantum Chem.*, **16**, 615–622 (1979).

(60) M. M. Dhingra and R. H. Sarma in "Stereodynamics of Molecular Systems", R. H. Sarma, Ed., Pergamon Press, New York, 1979, pp 3–38.

(61) I. C. P. Smith, H. H. Mantsch, R. D. Lapper, R. Deslauriers, and T. Schleich in "The Jerusalem Symposia on Quantum Chemistry and Biochemistry", Vol. 5, E. D. Bergmann and B. Pullman, Eds., The Israel Academy of Sciences and Humanities, Jerusalem, 1973, pp 381–402.

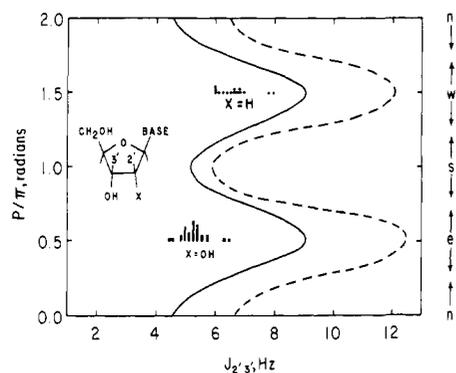(62) C.-H. Lee and R. H. Sarma, *J. Am. Chem. Soc.*, **98**, 3541–3548 (1976).

Figure 3. Theoretical dependence of the cisoidal proton coupling constant $J_{2'3'}$ upon P in ribose (solid curve) and deoxyribose (dashed path). Experimental values of $J_{2'3'}$ are represented by blocked (ribose) and dotted (deoxyribose) bar graphs. Relevant protons are noted in the chemical structure.

Table III. Comparison of Calculated and Experimental Coupling Constants (Hz) in Ribose

method	$J_{1'2'}$	$J_{2'3'}$	$J_{3'4'}$	Σ^a
PCILO (Pu)	8.4	5.4	1.6	10.0
PCILO (Pyr)	1.6	5.0	8.7	10.3
SE1	0.2	5.0	10.3	10.5
SE2	4.7	5.4	4.6	9.3
CFF	4.6	6.2	6.0	10.6
H	6.0	7.1	6.3	12.3
NMR data[11−13,22−26]	3.0–6.0	~5.0	6.0–3.0	9.0–10.0

^{a} Defined in text.

the deoxyribose data by dots. No differences in $J_{2'3'}$ are observed between the conformationally "rigid" 3′–5′ cyclic monophosphates[26,60,62] and unconstrained sugar systems;[11−13,22−29] the ribose data, however, are approximately 1–2 Hz lower in magnitude than the deoxyribose measurements. According to unpublished quantum mechanical calculations by Dr. I. Ekiel, the $J_{2'3'}$ coupling constant for ribose may be approximated with reasonable accuracy by a Karplus relationship; the ribose curve in Figure 3 is obtained from eq 5 with A, B, and C fixed at the above cited values and ϕ varied in accordance with available X-ray data. The quantum mechanical variation of $J_{2'3'}$ in β-deoxyribose, however, is similar to the slightly asymmetric path reported previously for α-deoxyribose[59] and thus reproduced here. According to these computations, the absence of the hydroxyl group at $C_{2'}$ is responsible for the asymmetry of the curve and also for the increased magnitude of $J_{2'3'}$ values in deoxyribose compared to those for ribose. As evident from Figure 3, for both ribose and deoxyribose sugars $J_{2'3'}$ is smallest in the n and s quadrants and greatest in the e and w ranges of pseudorotation space. The experimental $J_{2'3'}$ data are clustered at and, in the case of deoxyribose, sometimes even below the lowest theoretical values. The measured values are clearly indicative of minor e and w pseudorotation populations in solution.

The theoretically predicted dependence of the cisoidal $J_{1'2''}$ and the transoidal $J_{2''3'}$ coupling constants of deoxyribose are presented for the cycle of P in Figure 4. Experimental data and P states are represented exactly as in Figure 2. The $J_{1'2''}$ values are estimated from the $J_{1'2'}$ cisoidal constants computed for α-deoxyribose;[59] the variation of $J_{1'2''}$ with P in Figure 4 is out of phase
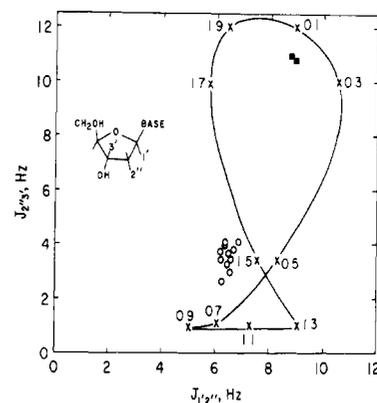

Figure 4. Theoretical dependence of the cisoidal $J_{1'2''}$ and the transoidal $J_{2''3'}$ proton coupling constants with P in deoxyribose. Experimental data are represented by open circles (free sugars) and darkened squares (3′–5′ cyclic monophosphates). Values of P/π are denoted by X, and relevant protons are indicated in the chemical structure.

by π rad from that reported for the α-deoxyribose system. The transoidal $J_{2''3'}$ data are obtained by using eq 5 with A, B, and C fixed at the values used to compute the $J_{1'2'}$ deoxyribose coupling and with ϕ varied over the X-ray ranges. Like $J_{1'2'}$ noted above, the $J_{2''3'}$ parameter is subject to electronegativity effects.[10,11] As evident from the diagram, the experimental data are positioned slightly off the path of deoxyribose pseudorotation. The data for the unconstrained sugars are consistent with a weighted blend of puckered states as detailed below. The couplings observed in 3′–5′ cyclic monophosphates[26,61,62] ($J_{1'2''} \approx 9$ Hz; $J_{2''3'} \approx 11$ Hz) are close to those expected for the $P \approx 0.2\pi$ rad structure observed in the solid state and are taken as calibration points of the $J_{1'2''}/J_{2''3'}$ curve.

Theory vs. Experiment in Solution

Ribose. Mean coupling constants computed on the basis of the various pseudorotation potential energy surfaces are presented in Tables III and IV. As evident from Table III, only the SE2 computations are able to account for the $J_{1'2'}$, $J_{2'3'}$, and $J_{3'4'}$ values observed in ribonucleosides and nucleotides (cf. Figures 2 and 3). Although the $J_{2'3'}$ data can be reproduced by the PCILO and SE1 approaches, it is not possible to reconcile the $J_{1'2'}$ and $J_{3'4'}$ data with the predicitons of these studies. On the other hand, the $J_{2'3'}$ values predicted by the CFF and H approaches are outside the range of experimental data while the computed $J_{1'2'}$ and $J_{3'4'}$ values are within acceptable limits. The value of $\Sigma = J_{1'2'} + J_{3'4'}$ computed on the basis of the H data, however, is far above the observed range of values. In accordance with conclusions derived elsewhere,[22] the experimental values of $J_{2'3'}$ and Σ in ribose are consistent with an energy barrier high enough (~2.2 and 6.0 kcal/mol according to the SE2 and PCILO data, respectively) to suppress intermediate conformers between the n and s ranges of pseudorotation space; the observed values of $J_{1'2'}$ and $J_{3'4'}$ are indicative of a blend of these two domains in approximately equal proportions.

Deoxyribose. According to the compilation in Table IV none of the pseudorotation studies reported to date can account for all five measured coupling constants in deoxyribonucleosides and -nucleotides (cf. Figures 2–4). Only the PCILO surfaces and the H data correctly predict $J_{1'2'}$ to exceed $J_{3'4'}$. While the H computations are closest to match the observed values of $J_{1'2'}$ and $J_{3'4'}$,

Table IV. Comparison of Calculated and Experimental Coupling Constants (Hz) in Deoxyribose

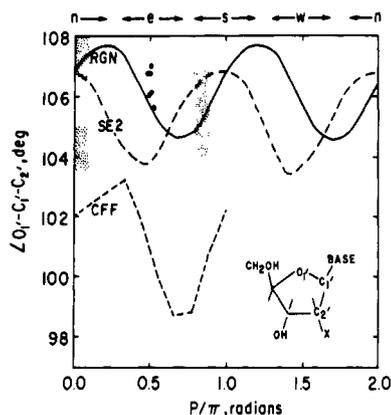| method	$J_{1'2'}$	$J_{1'2''}$	$J_{2'3'}$	$J_{2''3'}$	$J_{3'4'}$	Σ^a
PCILO (Pu)	9.4	6.1	6.4	2.4	1.3	10.7
PCILO (Pyr)	6.3	7.1	6.7	6.2	4.9	11.2
SE2	5.0	7.1	7.3	7.1	5.1	10.1
CFF	5.5	7.8	8.5	7.0	6.5	12.0
H	9.3	6.8	9.6	3.0	4.3	13.6
NMR data[11,25−29]	7.0–8.0	6.0–7.0	6.0–7.0	3.0–4.0	3.0–4.0	10.0–11.0

^{a} Defined in text.

Figure 5. Dependence of the $O_1{-}C_1{-}C_2$ valence angle with P associated with CFF and SE2 energy analyses (dashed curves) and observed in X-ray studies. The solid RGN curve was determined by a regression analysis of relevant experimental data.[7] Observed valence angles are represented in n and s quadrants by shaded areas and in the e quadrant by heavy dots. The valence angle is distinguished in the chemical structure.

Figure 6. Dependence of the $C_3{-}C_4{-}O_1$ valence angle with P. See legend to Figure 5.

these data fail to reproduce $J_{2'3'}$ and $\sum$ correctly and to account for the nearly identical magnitudes of $J_{2''3'}$ and $J_{3'4'}$. The SE2 and CFF potential surfaces incorrectly predict $J_{3'4'}$ to exceed $J_{1'2'}$; the CFF data additionally fail to reproduce $J_{2'3'}$ while the SE2 study incorrectly indicates a significant difference in magnitude between $J_{2''3'}$ and $J_{3'4'}$. The various surfaces predict values of $J_{2''3'}$ either much larger or somewhat smaller than experimental observations; only the CFF data fail to approximate $J_{1'2''}$ satisfactorily. As suggested by earlier studies,[10,11,25-27] the principal states describing the conformation of deoxyribose in solution appear, on the basis of the ^{1}H NMR data, to be a weighted blend of n and s conformers. Comparison of the computations with experimental $J_{2'3'}$ and $\sum$ values suggests the intermediate e domain to be fairly high in energy; in accordance with the successful predictions of these two parameters by PCILO and SE2 studies, the pseudorotation barrier lies somewhere between 1.5 and 5.0 kcal/mol above the global energy minimum. The correspondence of theory with the observed values of $J_{1'2'}$, $J_{2''3'}$, and $J_{3'4'}$ indicates that this minimum falls in the s domain. The energy difference between n and s domains appears, on the basis of the more successful predictions (PCILO and H) of these last three parameters, to be between 0.5 and 3.0 kcal/mol.

Geometric Comparisons

A final test of the reliability of the various pseudorotation potential surfaces is the degree to which the theoretical systems mimic standard molecular geometries of the furanose. According to recent analyses of the X-ray literature,[6-9] the endocyclic and exocyclic valence angles of ribose and deoxyribose depend upon the puckering of the sugar. Furthermore, according to regression analyses carried out first by Murray-Rust and Motherwell,[7] and later by de Leeuw et al.[8] and Westhof and Sundaralingam,[9] these angular variations appear to follow periodic functions linked to the phase angle of pseudorotation. Endocyclic bond lengths do not vary significantly with ring pucker while certain exocyclic bond lengths ($C_1{-}N$, $C_2{-}O_2$, and $C_3{-}O_3$) show differences of 0.03 Å with P.[8,9]

Selected internal valence angles associated with the SE2 and CFF analyses of deoxyribose are plotted as a function of P in Figures 5-7. The CFF parameters were computed by us from a table of corrected Cartesian coordinates supplied by M. Levitt for conformers over the range $P = 0{-}\pi$ rad. (The Cartesian coordinates reported in the original CFF study[30] are erroneous and are *not* the basis of the CFF energies. The unusual valence angles described by the erroneous coordinates have been noted by others.[8,9]) The SE2 data were reported by Broyde and Hingerty[38] in an application of the SE2 potential to selected dideoxynucleoside monophosphates. Unfortunately, valence angles are not reported in the other computations of pseudorotation
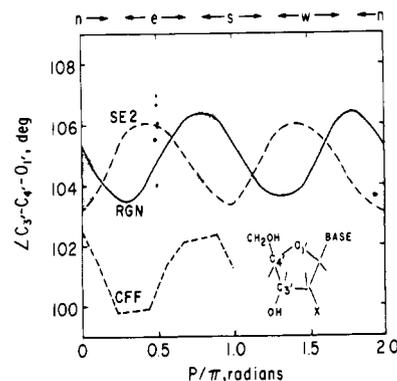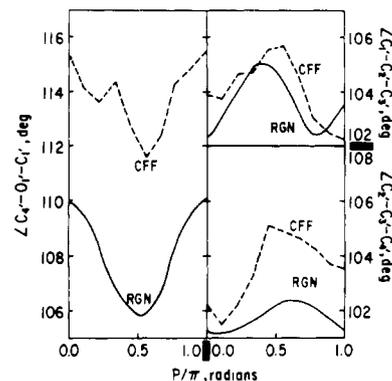

Figure 7. Dependence of the $C_4{-}O_1{-}C_1$, $C_1{-}C_2{-}C_3$, and $C_2{-}C_3{-}C_4$ valence angles with P in CFF and experimental (RGN) systems. See legend to Figure 5.

energy, and the SE2 data are limited to two variable valence angles.[63] The theoretical geometries of the SE2 and CFF systems are compared in Figures 5 and 6 with experimental data characterizing the six known e-puckered furanoses[15-21] and with the periodic functions (RGN) determined by the direct regression analyses of Murray-Rust and Motherwell[7] and Westhof and Sundaralingam.[9] The regression curves derived by de Leeuw et al.[8] on a larger data base with additional constraints of ring closure are somewhat discrepant from the RGN data cited here. The differences in the solid-state analyses, however, are minor compared to those noted between theory and experiment. For simplicity, the range of observed valence angles in the n and s quadrants of the two figures is represented by the shaded areas. The values of the different valence angles reported in the e-puckered systems are specified by dots at the appropriate value of P/π.

As evident from Figure 5, the SE2 variations of the internal valence angle $O_1{-}C_1{-}C_2$ fit experimental data in n- and s-puckered systems. The SE2 curve, however, does not match any observed values of $O_1{-}C_1{-}C_2$ in e-puckered systems and cannot account for the apparent decrease in this parameter as P increases from 0 to π rad. The SE2 curve lags by 0.2π rad behind the RGN curve designed on the basis of the experimental data. The fluctuations in $O_1{-}C_1{-}C_2$ described by the two curves, however, are similar in magnitude. The variation of $O_1{-}C_1{-}C_2$ with P in the CFF analyses, on the other hand shows major differences from the SE2 and RGN curves. The CFF curve matches no experimental data and involves values of $O_1{-}C_1{-}C_2$ significantly distorted from standard values. The sinusoidal variation of the CFF values, however, parallels that of the RGN curve.

The SE2 and RGN curves describing the variation of the $C_3{-}C_4{-}O_1$ valence angle with P in Figure 6 are out of phase by

---

(63) According to Westhof and Sundaralingam,[9] in the early SE2 and PCILO calculations, the geometry of some arbitrary preferred puckered state was used throughout the pseudorotation path without due consideration of the geometrical variations accompanying pseudorotation.

0.3π rad. The SE2 curve is able to match experimental observations in n- and e-puckered crystals but is located somewhat below the range of $C_3\text{-}C_4\text{-}O_1$, observed in s systems. The values of this parameter predicted by CFF energy minimization are consistently about 4° smaller than the experimental data. The magnitudes of angular fluctuations in the CFF analysis, however, are comparable to those predicted by the SE2 minimization and seen in the RGN curve. The variations of the CFF curve are also in phase with the RGN curve.

The CFF values of the endocyclic valence angles $C_4\text{-}O_1\text{-}C_1$', $C_1\text{-}C_2\text{-}C_3$', and $C_2\text{-}C_3\text{-}C_4$' are compared with the corresponding RGN curves in Figure 7. These valence angles are found in the SE2 computations to mimic the observed fluctuation of values illustrated by the RGN curve in Figure 7. (The theoretical variations in the $C_4\text{-}O_1\text{-}C_1$', $C_1\text{-}C_2\text{-}C_3$', and $C_2\text{-}C_3\text{-}C_4$' angles, however, are out of phase with the corresponding RGN curves and the predicted ranges of $C_1\text{-}C_2\text{-}C_3$' and $C_2\text{-}C_3\text{-}C_4$' are somewhat broader than indicated by the RGN analysis.[36]) The variable $C_4\text{-}O_1\text{-}C_1$' angles in the CFF study are consistently 5–6° greater than experimental data represented by the RGN curve over the range of P. Experimental fluctuations in this parameter, however, are approximately comparable and also parallel to those predicted by the CFF study. The CFF variations of $C_1\text{-}C_2\text{-}C_3$' and $C_2\text{-}C_3\text{-}C_4$', however, are greater than the experimental variations.[6-9] The CFF and RGN descriptions of $C_1\text{-}C_2\text{-}C_3$' are coincidental at $P = 0.3\pi$ and 0.8π rad while the two $C_2\text{-}C_3\text{-}C_4$' curves are most similar near $P = 0.1\pi$ rad. The $C_2\text{-}C_3\text{-}C_4$' CFF curve is parallel to the RGN observations but the $C_1\text{-}C_2\text{-}C_3$' CFF and RGN variations are out of phase by approximately 0.2π rad. Bond lengths are also permitted to relax in the CFF pseudorotation analysis. The variations of these parameters from standard values, however, are no greater than the 0.03-Å deviations observed in X-ray crystal structures.

The extreme fluctuations in valence bond angles may account for the unusual energetic profile of pentose pseudorotation in the CFF study. In computations described in the paper that follows,[64] we find the pseudorotation energy to depend dramatically upon such major (4–6°) deviations of internal valence angles. The computed energy is much less sensitive to the smaller (1–2°) angular distortions associated with the SE2 model. Variations in the $C_4\text{-}O_1\text{-}C_1$' valence angle, for example, affect the distances and nonbonded interactions between the bulky chain backbone and base moieties attached respectively to atoms C_4' and C_1' of the furanose. Indeed, for deoxyribose the e range of puckering becomes predominant as the $C_4\text{-}O_1\text{-}C_1$' angle increases to the unusually high values associated with the CFF computations in Figure 7. The flat potential surface of the CFF study depends, in addition, upon the relatively flat threefold torsional barriers utilized in CFF computations. These flat barriers usually compensate for the relatively large van der Waals radii and high nonbonded energy barriers associated with the CFF potential.[65] (For comparison, the torsional barriers are higher, the van der Waals radii shorter, and the nonbonded energy lower in SE2 computations.) With the unusual geometry employed in the CFF study above, both nonbonded and torsional energies of the e domain are small and consequently the barrier to pseudorotation between n and s states is negligible.

Concluding Remarks

The above comparisons of theoretical energies with experimental data shed new light upon the conformational role of the furanose in the nucleic acid backbone. The distinctly different behavior of model ribose and deoxyribose systems reveals some of the subtle influences of chemical architecture upon the three-dimensional structure of the nucleic acids. The simple substitution of the 2'-hydroxyl group in ribose by hydrogen in deoxyribose alters both the conformational preferences and the rate of pseudorotation between differently puckered states. The quasi-symmetric ribose

ring (described with respect to the mirror plane that passes through O_1' and bisects the $C_2\text{-}C_3$' bond in Figure 1) favors n- and s-puckered sugars with almost equal likelihood both in the solid state and in solution. According to potential energies that reproduce these results,[34,36,64] interatomic contacts and molecular forces are virtually equivalent in the n- and s-puckered forms of ribose. More specifically, interactions involving the 3'-oxygen in one conformation approximately balance interactions associated with the 2'-hydroxyl in the other form (and vice versa); energies describing the influence of the 5'-CH_2OH moiety upon the ring similarly counteract interactions of the base with the sugar in the differently puckered states. The structurally asymmetric deoxyribose ring, however, exhibits a decided preference for s over n puckering in all experimental studies. Unfortunately, none of the potential energy surfaces reported to date provides any structural rationale behind this behavior.[32,35] Theoretical analyses described in the accompanying paper[64] reveal that the s preference of deoxyribose pseudorotation stems from so-called "gauche" effects in the structure. The available X-ray data[6-9] together with the reported NMR coupling constants[10-13] also suggest that the transition between different puckerings is more difficult in ribose than in deoxyribose. Theoretical results offered until now ascribe this difference solely to the greater nonbonded energy involving the relatively large hydroxyl group of ribose compared to the small hydrogen of deoxyribose.[34,36] Calculations presented in the accompanying paper[64] demonstrate that the extra "stiffness" of ribose pseudorotation stems, in addition, from gauche effects associated with the 2'-hydroxyl moiety.

According to these computations, no theoretical study has yet succeeded in reproducing the experimental descriptions of both ribose and deoxyribose pseudorotation. Classical semiempirical potential functions[33,34,36-38] that successfully account for X-ray and NMR measurements of ribose flexibility fail to rationalize similar studies involving deoxyribose. The similar nonbonded energies of n and s states in semiempirical studies explain the observed blend of ribose conformers. The classical nonbonded potential, however, incorrectly favors the sterically less hindered n conformer over the experimentally preferred s state in deoxyribose. While closely related to classical semiempirical potential functions, the consistent force field studies reported to date[30] fail to describe either ribose or deoxyribose conformations correctly. As noted above, these errors may stem from the utilization of anomalous geometries. With structures of comparable geometry, consistent force field energies usually mimic semiempirical potential surfaces.[65] The quantum mechanical PCILO approach,[35] on the other hand, matches the experimental descriptions of deoxyribose in the solid state and in solution but incorrectly predicts base sequence dependent conformational effects in ribose. The composite PCILO description of purine and pyrimidine ribonucleosides, however, fits experimental observations fairly accurately. As a consequence of unusually low potential barriers, Hückel[32] pseudorotation energies also do not reproduce the experimental behavior of the furanose. If these barriers were greater in magnitude, the Hückel approach would successfully describe the n/s conformational preferences of both ribose and deoxyribose.

In view of the various uncertainties of computations at the monomer level, theoretical pseudorotation analyses in larger nucleic acid systems must be regarded with some reservations. According to minimization studies published to date, the energetically favored sugar conformations in large nucleic acid fragments are closely related to those predicted in corresponding nucleoside studies. For example, an unusually large number of low energy e-puckered conformers are found by Tosi and Rasmussen[66] upon application of a low pseudorotation barrier (consistent force field) potential to sugar–phosphate–sugar fragments. With use of the CFF potential analyzed above in the energy minimization of a 20 base pair segment of double-helical DNA, e puckerings are also preferred over n and s states for straight, twisted, and superhelical chains.[31] The e state is not favored, however, either in analogous semiempirical energy minimizations[37,38,67] or in experimental

(64) W. K. Olson, *J. Am. Chem. Soc.*, following article in this issue.
(65) A. T. Hagler, P. S. Stern, R. Sharon, J. M. Becker, and F. Naider, *J. Am. Chem. Soc.*, **101**, 6842–6852 (1979).

(66) C. Tosi and K. Rasmussen, *Biopolymers*, **20**, 1059–1088 (1981).

How Flexible Is the Furanose Ring

J. Am. Chem. Soc., Vol. 104, No. 1, 1982 277

studies of ordinary oligo- and polynucleotides.[4,13,43,68-83] In the semiempirical studies the n state is consistently favored over the s regardless of sugar type. This prediction is supported by experimental studies on oligo- and polyribonucleotides[13,43,70,72,75-83] but is contradicted by findings for large deoxyribose systems,[4,68-71,73,74] where s is favored. The latter discrepancy has been attributed by others to the absence of solvent effects in the semiempirical computations;[36,67] this hypothesis is based on the fact that DNA fibers at low humidity and low salt content occur as A-family helices with n-type sugar puckering.[4,5] According to the analysis presented here, some of the computed preference for n over s conformers in deoxyribose oligomers is a consequence of inconsistencies in the semiempirical potential at the nucleoside level. The predominance of the n pucker in the semiempirical energy analyses of both RNA and DNA oligomers is related, in addition, to the structural asymmetry that accompanies the incorporation of either ribose or deoxyribose into the polynucleotide backbone together with certain approximations in the semiempirical potential energy functions. Beyond the monomer level the nonbonded interactions involving the base and 2'-substituent are no longer balanced by interactions involving the 5'- and 3'-sugar moieties, respectively. At the oligomer level, the nonbonded stacking interactions involving sequential bases are the major determinants of computed semiempirical potential energies. Because base stacking is more extensive with n puckering, an n-puckered chain is computationally favored over an s-puckered chain regardless of sugar chemistry. Unfortunately, the potential energy function commonly used to describe the nonbonded interactions of the nucleotide bases and backbone is designed to describe model peptides and is not scaled to reproduce base stacking contacts and interactions. Semiempirical functions that account for base-stacking geometries[84] are appreciably different from those reported in the semiempirical oligomer minimization studies.[37,38,67] Energy minimizations based upon semiempirical potential functions developed to reproduce properties of nucleic acid analogues (e.g., pseudorotation, stacking, etc.) are expected to differ appreciably from energy predictions now in the biophysical literature.

Our comparisons of experiment with theory also demonstrate that the pseudorotation of ribose and deoxyribose is not "free" as recently suggested.[30] According to both the computed potential energies and the available X-ray data, the pentose oscillates between n and s puckerings via the e quadrant of intermediate states rather than over the entire range of pseudorotation space; excessive potential energies disfavor the intermediate w range in all reported surfaces. The theoretical studies that best reproduce NMR coupling constants further suggest that the potential barrier in the e quadrant lies between 2 and 5 kcal/mol above the global minimum. Such energies are sufficiently high to suppress intermediate forms but low enough to permit the rapid interconversion of n and s states. The presence of energy barriers substantially exceeding RT, where R is the gas constant and T the absolute temperature, substantiates conventional analyses of nucleic acid conformation in terms of the two predominant sugar puckerings.[4,10,13,43,71,72,85] (In certain chemically damaged nucleosides, however, the pseudorotation barrier essentially disappears and the usual two-state model fails.[54]) Like a C–C single bond, the furanose ring of normal DNA and RNA adopts a limited number of spatial arrangements. In analogy to single bonds, the sugar additionally fluctuates within its few preferred domains to assume optimal spatial arrangements.

The restricted motions of the pentose ultimately limit the flexibility of the polynucleotide as a whole. The sugars of the polynucleotide apparently flip in steplike jumps between n and s conformers rather than vary gradually through intermediate pseudorotation ranges. Indeed, almost all large nucleic acid structures refined to date[81-83,86-88] adopt the two standard furanose puckers. The variations among the many X-ray examples arise from different combinations of n/s puckering (i.e., all-n, all-s, or mixed n/s) coupled with systematic variations of acyclic rotations in the sugar phosphate backbone.[4] The questions of unusual sugar flexibility recently raised in the exciting single-crystal X-ray studies of large DNA fragments[89,90] may possibly reflect the potential energy restraints utilized in the least-squares refinement. Systems such as these, in which the crystallographic data are not to high enough resolution to determine sugar pucker unequivocally, require additional information in the form of an energy function to make the X-ray least-squares refinement converge.[91] The examples of unusual sugar puckering reported by Drew et al.[89] in the Z-DNA dCGCG self-complementary duplex and by Wing et al.[90] in a complete B-DNA double-helical turn of dCGCGAATTCGCG interestingly derive from a refinement procedure that utilizes the same unusually free CFF pseudorotation potential questioned here. In contrast, only the two common sugar conformations appear in the four different crystals of the dCGCGCG duplex obtained by Wang et al.[87,88] with a different restrained refinement procedure. In view of the present analysis of pseudorotation potentials, one not only questions the extent to which the restrained refinement procedures determine the reported sugar conformation but also ponders the significance, if any, of the unusually puckered models.

Finally, the distribution of n/s puckering together with the rate of pseudorotation distinguishes RNA from DNA. The extra "stiffness" of ribose pseudorotation seems to impart some of the stability required for folding long RNA chains. The n-puckered riboses of the polyribonucleotides may play a structural role somewhat analogous to the rigid planar trans peptide moieties of the polypeptides. The enhanced flexibility of the deoxyribose

(67) S. Broyde and B. Hingerty, *Nucleic Acids Res.*, **6**, 2165–2178 (1979).

(68) F. K. Fang, N. S. Kondo, P. S. Miller, and P. O. P. Ts'o, *J. Am. Chem. Soc.*, **93**, 6647–6656 (1971).

(69) J. L. Alderfer and S. L. Smith, *J. Am. Chem. Soc.*, **93**, 7305–7314 (1971).

(70) N. S. Kondo, K. N. Fang, P. S. Miller, and P. O. P. Ts'o, *Biochemistry*, **11**, 1991–2003 (1972).

(71) D. M. Cheng and R. H. Sarma, *J. Am. Chem. Soc.*, **99**, 7333–7348 (1977).

(72) F. S. Ezra, C.-H. Lee, N. S. Kondo, S. S. Danyluk, and R. H. Sarma, *Biochemistry*, **16**, 1977–1987 (1977).

(73) N. Carmerman, J. K. Fawcett, and A. Camerman, *J. Mol. Biol.*, **107**, 601–621 (1976).

(74) M. A. Viswamitra, O. Kennard, P. G. Jones, G. M. Sheldrick, S. Salisbury, L. Falvello, and Z. Shakked, *Nature (London)*, **273**, 687–688 (1978).

(75) J. L. Sussman, N. C. Seeman, S.-H. Kim, and H. M. Berman, *J. Mol. Biol.*, **66**, 403–421 (1971).

(76) J. Rubin, T. Brennan, and M. Sundaralingam, *Biochemistry*, **11**, 3112–3228 (1972).

(77) D. Suck, P. C. Manor, G. Germain, C. H. Schwalbe, G. Weimann, and W. Saenger, *Nature (London), New Biol.* **246** 161–165 (1973).

(78) N. C. Seeman, J. M. Rosenberg, F. L. Suddath, J. J. P. Kim, and A. Rich, *J. Mol. Biol.*, **104**, 109–144 (1976).

(79) J. M. Rosenberg, N. C. Seeman, R. O. Day, and A. Rich, *J. Mol. Biol.*, **104**, 145–167 (1976).

(80) B. Hingerty, E. Subramanian, S. D. Stellman, T. Sato, S. B. Broyde, and R. Langridge, *Acta Crystallogr., Sect. B*, **B32**, 2998–3013 (1976).

(81) B. Hingerty, R. S. Brown, and A. Jack, *J. Mol. Biol.*, **124**, 523–534 (1978).

(82) J. L. Sussman, S. R. Holbrook, R. W. Warrant, G. M. Church, and S.-H. Kim, *J. Mol. Biol.*, **128**, 607–630 (1978).

(83) C. D. Stout, H. Mizuno, S. T. Rao, P. Swaminathan, J. Rubin, T. Brennan, and M. Sundaralingam, *Acta Crystallogr., Sect. B*, **B34**, 1529–1544 (1978).

(84) W. K. Olson, *Biopolymers*, **17**, ,1015–1040 (1978).

(85) W. K. Olson and P. J. Flory, *Biopolymers*, **11**, 1–23 (1972).

(86) A. Klug, A. Jack, M. A. Viswamitra, O. Kennard, Z. Shakked, and T. A. Seitz, *J. Mol. Biol.*, **131**, 669–680 (1979).

(87) A. H.-J. Wang, G. J. Quigley, F. J. Kolpak, J. L. Crawford, J. H. van Boom, G. van der Marel, and A. Rich, *Nature (London)*, **282**, 680–686 (1979).

(88) A. H.-J. Wang, G. J. Quigley, F. J. Kolpak, G. van der Marel, J. H. van Boom, and A. Rich, *Science (Washington, D.C.)*, **211**, 171–176 (1981).

(89) H. Drew, T. Takano, S. Tanaka, K. Itakura, and R. E. Dickerson, *Nature (London)*, **286**, 567–573 (1980). The $C_{1'}$-exo conformation reported in this structure has been termed a "slightly bent $C_{2'}$-endo" form and is better classified as s puckered rather than e puckered.

(90) R. Wing, H. Drew, T. Takano, C. Broka, S. Tanaka, K. Itakura, and R. E. Dickerson, *Nature (London)*, **287**, 755–758 (1980). At the preliminary refinement stage reported here, the pucker is distributed equally between s and e conformers.

(91) J. L. Sussman, S. R. Holdbrook, G. M. Church, and S.-H. Kim, *Acta Crystallogr., Sect. A*, **A33**, 800–804 (1977).

ring, on the other hand, may enhance the interconversions between the many helical forms of DNA. The pseudorotation of deoxyriboses in the DNA backbone remotely resembles the cis/trans peptide rotation that accompanies the I/II helical transformation in poly-L-proline. The distinctly different pseudorotation of the ribose and deoxyribose thus appears to be a general feature that characterizes the respective polynucleotides and that influences their recognition by various molecular agents.

Supplementary Material Available: Bibliographies of ribose and deoxyribose structures (Tables I-S and II-S) (12 pages). Ordering information is given on any current masthead page.

How Flexible Is the Furanose Ring? 2. An Updated Potential Energy Estimate

Wilma K. Olson

Contribution from the Department of Chemistry, Rutgers University, New Brunswick, New Jersey 08903. Received November 25, 1980

Abstract: A potential energy function is developed to estimate the pseudorotational motions of ribose and 2'-deoxyribose sugars. In addition to standard nonbonded, torsional, and valence angle strain contributions, an intrinsic gauche energy term is required to account for the puckering preferences and hindered ring flexibilities suggested by solid-state and solution studies. The gauche effect is also found to be an essential factor in reproducing the properties of 3'-deoxyribose and 2'-fluoro-2'-deoxyribose rings in solution. The extreme sensitvity of the potential energies to variations in ring geometry is helpful in understanding the disparities noted in 1 among earlier theoretical studies of furanose pseudorotation.[1] Apparently minor deviations of valence bond angles from standard X-ray values are found to perturb the normal motions of the furanose drastically.

Introduction

The inadequacy of theories to account satisfactorily for the physical properties of nucleic acids prompted the present reinvestigation of furanose pseudorotation. The comparative study detailed in the preceeding paper,[1] hereafter referenced as 1, reveals serious discrepancies between published potential energy surfaces and experimental observations of sugar puckering. No single potential method offered to date reproduces the unique conformational (puckering) preferences of different sugars (e.g., ribose and deoxyribose) and also mimics the known geometric (valence angle) changes that accompany furanose pseudorotation. Such discrepancies weaken the predictive value of theoretical work in bridging the gaps between experimental examples and also in extrapolating the behavior of low molecular weight nucleic acid analogues to long polynucleotide chains.

The difficulties in successful prediction of ribose and deoxyribose pseudorotation resemble conformational discrepancies found previously in several unrelated molecules constructed from the same chemical building blocks. The unexplained preference for certain pentose puckerings on the basis of steric and electrostatic forces alone parallels the anomalous predisposition of the O–C–C–C and O–C–C–O sequences in various polyoxides,[2,3] carbohydrates,[4-7] and smaller molecules[8-14] to adopt gauche in favor of trans rotational arrangements. This so-called "gauche" effect[15,16] characterizes a large assortment of compounds composed of atoms such as oxygen that possess unshared p electrons. According to quantum mechanical analyses,[17] the predisposition for gauche conformations in the aforementioned systems stems from stabilizing bond–antibond interactions involving the polar C–O linkages. The persistence of such effects in the furanose presumably influences the torsions of the five-membered ring and ultimately affects the potential energy of pseudorotation.

The computational improvements outlined below reconcile earlier discrepancies of semiempirical energy studies with the experimental properties of ribose and deoxyribose. The inclusion of gauche effects in the usual partitioned potential functions accounts at once for the unexplained puckering preferences of the different sugars. The extreme sensitivity of the potential energy function to internal ring geometry also helps to explain the disparities found in 1 among earlier theoretical estimates of pentose pseudorotation. Minor (2–3°) deviations of valence bond angles

(1) W. K. Olson and J. L. Sussman, *J. Am. Chem. Soc.*, preceding article in this issue.
(2) A. Abe and J. E. Mark, *J. Am. Chem. Soc.* **98**, 6468–6472 (1976).
(3) E. Riande and J. E. Mark, *Macromolecules*, **11**, 956–959 (1978).
(4) G. A. Jeffrey, J. A. Pople, and L. Radom, *Carbohydr. Res.*, **25**, 117–131 (1972); **38**, 81–95 (1974).
(5) A. Abe, *J. Am. Chem. Soc.*, **98**, 6477–6480 (1976).
(6) G. A. Jeffrey, J. A. Pople, J. S. Binkley, and S. Vishveshwara, *J. Am. Chem. Soc.*, **100**, 373–379 (1978).
(7) G. A. Jeffrey and R. Taylor, *J. Comput. Chem.*, **1**, 99–109 (1980).
(8) O. Bastiansen, *Acta Chem. Scand.*, **3**, 415–421 (1949).
(9) P. J. Krueger and H. D. Mettee, *J. Mol. Spectrosc.*, **18**, 131–140 (1965).
(10) P. Buckley and P. A. Giguère, *Can. J. Chem.*, **45**, 397–407 (1967).
(11) A. A. Abdurahmanov, R. A. Rahimova, and L. M. Imanov, *Phys. Lett. A*, **32A**, 123–124 (1970).
(12) H. Matsuura, M. Hiraishi, and T. Miyazawa, *Spectrochim. Acta, Part A*, **28A**, 2299–2304 (1972).
(13) L. Radom, W. A. Lathan, W. J. Hehre, and J. A. Pople, *J. Am. Chem. Soc.*, **95**, 695–698 (1973).
(14) W. K. Busfield, M. P. Ennis, I. J. McEwen, *Spectrochim. Acta, Part A*, **29A**, 1259–1264 (1974).
(15) E. L. Eliel and C. A. Giza, *J. Org. Chem.*, **33**, 3754–3758 (1968).
(16) S. Wolfe, *Acc. Chem. Res.*, **5**, 102–111 (1972).
(17) T. K. Brunck and F. Weinhold, *J. Am. Chem. Soc.*, **101**, 1700–1709 (1979).